RESEARCH ARTICLE

Impact of manganese on biofilm formation and cell morphology of *Candida parapsilosis* clinical isolates with different biofilm forming abilities

Sulman Shafeeq[1,*,†], Srisuda Pannanusorn[1,2], Youssef Elsharabasy[1], Bernardo Ramírez-Zavala[3], Joachim Morschhäuser[3] and Ute Römling[1,*,‡]

[1]Department of Microbiology, Tumor and Cell Biology, Karolinska Institutet, SE-17165, Stockholm, Sweden, [2]Department of Biotechnology, Faculty of Science and Technology, Thammasat University, 12120, Bangkok, Thailand and [3]Institute for Molecular Infection Biology, University of Würzburg, D-97080, Würzburg, Germany

*Corresponding author: Department of Microbiology, Tumor and Cell Biology, Biomedicum C8, Karolinska Institutet, Solnavägen 9, SE-17165, Stockholm, Sweden. E-mail: sulman.shafeeq@ki.se and ute.romling@ki.se

One sentence summary: Impact of manganese on biofilm formation in *Candida parapsilosis*.

Editor: Carol Munro
†Sulman Shafeeq, http://orcid.org/0000-0003-1152-526X
‡Ute Römling, https://orcid.org/0000-0003-3812-6621

ABSTRACT

The commensal species *Candida parapsilosis* is an emerging human pathogen that has the ability to form biofilms. In this study, we explored the impact of the divalent cations cobalt (Co^{2+}), copper (Cu^{2+}), iron (Fe^{3+}), manganese (Mn^{2+}), nickel (Ni^{2+}) and zinc (Zn^{2+}) on biofilm formation of clinical isolates of *C. parapsilosis* with no, low and high biofilm forming abilities at 30 and 37°C. All strains besides one isolate showed a concentration-dependent enhancement of biofilm formation at 30°C in the presence of Mn^{2+} with a maximum at 2 mM. The biofilm forming ability of no and low biofilm forming isolates was >2-fold enhanced in the presence of 2 mM Mn^{2+}, while the effect in high biofilm forming isolate was significantly less pronounced. Of note, cells in the biofilms of no and low biofilm forming strains differentiated into yeast and pseudohyphal cells similar in morphology to high biofilm formers. The biofilm transcriptional activator *BCR1* has a dual developmental role in the absence and presence of 2 mM Mn^{2+} as it promoted biofilm formation of no biofilm forming strains, and, surprisingly, suppressed cells of no biofilm forming strains to develop into pseudohyphae and/or hyphae. Thus, environmental conditions can significantly affect the amount of biofilm formation and cell morphology of *C. parapsilosis* with Mn^{2+} to overcome developmental blocks to trigger biofilm formation and to partially relieve *BCR1* suppressed cell differentiation.

Keywords: *Candida parapsilosis*; biofilm formation; metal ions; manganese; *BCR1*; yeast cells; pseudohyphae; hyphae; cell morphology

INTRODUCTION

A primary cause of morbidity and mortality in hospitals is nosocomial fungal infections due to *Candida* species. Nosocomial bloodstream infections have *Candida* species as the fourth most common causative agent with *Candida albicans* as the most common species isolated from these infections (Wisplinghoff *et al.* 2004). The frequency of invasive infections by non-albicans *Candida* species especially *Candida parapsilosis* has increased over the past few decades (Tóth *et al.* 2019), with *C. parapsilosis* often being the second most commonly isolated species from bloodstream infections (Pfaller *et al.* 2011). However, *C. parapsilosis* can sometimes even become the leading cause of *Candida* infections in hospitals around the globe (Ng *et al.* 2001; Pfaller *et al.* 2001; Medrano *et al.* 2006; Tóth *et al.* 2019). In one-fourth of fungal infections in newborns with low weight in the United Kingdom, *C. parapsilosis* is the causative agent of mortality in neonatal intensive care units (Roilides *et al.* 2004; Clerihew *et al.* 2007; Tóth *et al.* 2019).

Typically, *C. parapsilosis* is not an obligate human pathogen, but a harmless commensal of the human skin (Weems 1992). However, the hands of healthcare workers colonized by *C. parapsilosis* are the most relevant source of transmission and outbreaks in hospitals, when infecting susceptible individuals (Kuhn *et al.* 2004). *Candida parapsilosis*, though, is more widespread and has also been isolated in nature from sources such as animals, soil and insects (Trofa, Gácser and Nosanchuk 2008). This species is notorious for its capacity to form biofilms on catheters and other implanted devices (Trofa, Gácser and Nosanchuk 2008; van Asbeck, Clemons and Stevens 2009). Therefore, patients with prolonged use of a central venous catheter or other indwelling devices are at increased risk for infection with *C. parapsilosis* (Trofa, Gácser and Nosanchuk 2008). The ability to form biofilms has been considered to be an important, if not the major, virulence factor of *C. parapsilosis*.

In *C. albicans*, systematic analyses identified the gene network regulating biofilm formation. Especially, a panel of transcription factors has been demonstrated to play a predominant role in the regulation of biofilm formation in *C. albicans* (Finkel and Mitchell 2011; Nobile *et al.* 2012; Araújo, Henriques and Silva 2017). Bcr1, a major biofilm transcriptional regulator of *C. albicans*, was shown to have a differential role in biofilm formation of *C. parapsilosis* (Ding and Butler 2007; Ding *et al.* 2011). While Bcr1 promotes biofilm formation in low biofilm forming isolates of *C. parapsilosis* (Pannanusorn *et al.* 2014), it does not trigger biofilm formation in high biofilm forming isolates of *C. parapsilosis* (Pannanusorn *et al.* 2014). Also, other transcriptional factors can have distinct roles in *C. parapsilosis*. For example, Ume6 does not have a major effect on biofilm formation in *C. albicans*, but significantly promotes biofilm formation in *C. parapsilosis* (Holland *et al.* 2014; Araújo, Henriques and Silva 2017).

Metal ions are vital for microorganisms, as they are required to perform fundamental biological processes such as DNA replication, transcription, biosynthesis of precursors, respiration and the oxidative stress response (Allison *et al.* 2016). Nevertheless, the full spectrum of biological functions of metal ions has not been explored (Cvetkovic *et al.* 2010). The availability and biological functionality of metal ions vary widely (Mackie *et al.* 2016; Rodríguez and Mandalunis 2018). Metal ions also play a role in biofilm formation and cell morphology. In *C. albicans* and *Candida tropicalis*, various metal ions affected cell differentiation during biofilm growth (Harrison *et al.* 2007). *Candida albicans* biofilms are composed of yeast and hyphal cells (Odds 1988). Hyphal formation in biofilms of *C. albicans* was inhibited

by arsenic, cadmium, chromium, cobalt, copper, selenium, silver and zinc, while enhanced by lead (Harrison *et al.* 2007). Similarly, in *C. tropicalis* hyphal formation was enhanced by chromium and zinc, but inhibited by arsenic, cadmium, cobalt, copper, lead, selenium and silver (Odds 1988). The morphological transition from yeast to a pseudohyphal/hyphal form has an important role in the virulence of *C. albicans* and is affected by numerous environmental conditions (Odds 1988; Lackey *et al.* 2013). *Candida parapsilosis,* however, has not been considered to form true hyphae like *C. albicans* (Trofa, Gácser and Nosanchuk 2008). High biofilm forming strains of *C. parapsilosis* showed a morphologically distinct biofilm composed of yeast and pseudohyphae, while biofilms of low biofilm forming strains were composed of yeast cells (Pannanusorn, Fernandez and Römling 2013; Pannanusorn *et al.* 2014). *Candida parapsilosis* yeast cells have an oval, round or cylindrical shape suggesting different, noncategorized cell types (Trofa, Gácser and Nosanchuk 2008).

Previously, we have categorized clinical strains of *C. parapsilosis* from bloodstream infection into no, low and high biofilm formers (Pannanusorn *et al.* 2014). The concentration of divalent cations can vary widely in environmental settings and in the human body. Here, we explored the impact of enhanced concentrations of different essential divalent metal ions on the biofilm forming ability of selected clinical isolates of *C. parapsilosis*. Interestingly, we demonstrate that in the presence of 2 mM of the divalent manganese cation (Mn^{2+}) at 30°C, biofilm formation in no and low biofilm formers was consistently >2-fold enhanced and cells differentiated into yeasts and pseudohyphae. This enhanced biofilm forming ability of no biofilm formers in the presence of Mn^{2+} was dependent on Bcr1 with cell differentiation suppressed by Bcr1. Moreover, we identified the presence of hyphae, long thin filamentous cells with minimal constriction at the septal junction, mainly in the *bcr1*Δ mutant. In summary, Bcr1 has opposite effects on the amount of biofilm formation and differential cell morphology. Thus, Bcr1 is a transcriptional regulator of biofilm formation versus cell differentiation in *C. parapsilosis* pronounced under elevated Mn^{2+} concentration.

MATERIALS AND METHODS

Strains and growth conditions

Candida parapsilosis clinical isolates SMI 416, SMI 501, SMI 630, SMI 661, SMI 681, SMI 694, SMI 706, SMI 798 and SMI 828 from bloodstream infection (Pannanusorn, Fernandez and Römling 2013; Pannanusorn *et al.* 2014) and the reference strain ATCC 22019 from the American Type Culture Collection (Manassas, VA, USA) were used in this study (Table S1, Supporting Information). YPD agar plates (2% peptone, 1% yeast extract, 2% glucose and 1.5% agar) were used to grow *C. parapsilosis* for 48 h at 37°C. Single colonies were suspended in YNB medium (0.67% yeast nitrogen base, Sigma) supplemented with 2% glucose (YNB/2% glucose) and incubated overnight at 30 or 37°C depending on the incubation temperature in the next step. Divalent transition metal ions were added as a salt of nitrate ($Co(NO_3)_2$, $Cu(NO_3)_2$, $Fe(NO_3)_3$, $Mn(NO_3)_2$, $Ni(NO_3)_2$ and $Zn(NO_3)_2$) at different concentrations as indicated. In YNB medium, Mn^{2+} concentration of 2.367 μM (manufacturer information) was set as 0 mM.

*bcr1*Δ mutant construction

A *bcr1*Δ mutant was constructed in the clinical isolate SMI 416 and the reference strain ATCC 22019. Construction of the *BCR1*

deletion and complementation of the *bcr1Δ* mutant was performed by using the SAT1 flipping strategy (Reuss *et al.* 2004; Sasse and Morschhäuser 2012). The *bcr1* deletion mutant plasmid pBCR1CpM2 constructed previously (Pannanusorn *et al.* 2014) was used for two sequential rounds of transformation and recycling of the cassette to delete *bcr1* on both chromosomes. Two independent *bcr1Δ* mutants were constructed for each strain. For complementation of the ATCC 22019 *bcr1Δ* mutant, pBCR1CpMK1 (Pannanusorn *et al.* 2014) was integrated into one of the *bcr1Δ* alleles of the homozygous mutant, followed by recycling of SAT1 flipper cassette. All deletion events and the complementation were verified by Southern blotting using the *BCR1* upstream fragment as the hybridization probe.

Biofilm formation

Biofilms were allowed to form in presterilized polystyrene flat-bottom 96-well microtiter plates in the presence of different concentrations of metal ions in YNB/2% glucose. Wells of the microtiter plate were inoculated with 200 μl cell suspension ($OD_{600} = 0.1$) in YNB/2% glucose medium without or with the desired concentration of the divalent metal ion. Cobalt (Co^{2+}), copper (Cu^{2+}), iron (Fe^{3+}), manganese (Mn^{2+}), nickel (Ni^{2+}) and zinc (Zn^{2+}) were used at 0.1, 0.2, 0.5, 1, 2 and 10 mM concentration as a salt of nitrate. To allow yeast cells to adhere to the polystyrene surface of the well, the plates were incubated at 30 or 37°C for 3 h. After the adhesion phase, the cell suspension was removed and each well was washed three times with 250 μl fresh medium (without added glucose and metal ion). Fresh YNB/2% glucose medium (200 μl) without or with the desired concentration of metal ion was added in each well. The plates were incubated at 30 or 37°C for 48 h.

Crystal violet assay

Biofilm formation was quantified by the crystal violet assay (O'Toole 2011). For the crystal violet assay, wells with developed biofilms were washed three times with 250 μl PBS (1×). Then, wells were stained with 200 μl 0.2% crystal violet (Sigma) for 10 min. Stained wells were washed three times with 250 μl sterilized distilled water. Wells were destained with 200 μl 30% acetic acid. The dissolved crystal violet was quantified by measuring the absorbance at 600 nm.

Assessment of cell morphology in biofilms

To assess cell morphology in surface attached biofilms, *C. parapsilosis* was grown in presterilized polystyrene flat-bottom 24-well microtiter plates to produce biofilms in the presence of YNB/2% glucose medium with and without 2 mM Mn^{2+} at 30°C. Each well of the microtiter plate was inoculated with 1 ml cell suspension ($OD_{600} = 0.1$) in YNB/2% glucose medium without or with 2 mM Mn^{2+}. Yeast cells were allowed to adhere for 3 h. After the adhesion phase, the cell suspension was removed and each well was washed three times with 2 ml fresh medium without Mn^{2+}. Fresh YNB/2% glucose medium (1 ml) without or with 2 mM Mn^{2+} was added in each well. The plates were incubated at 30°C for 48 h. After 48 h, biofilm wells were washed three times with 2 ml PBS (1×) and the cell morphology was investigated under the light microscope (Leica) with 20× magnification.

For confocal microscopy, *C. parapsilosis* was grown in presterilized polystyrene flat-bottom 24-well microtiter plates to produce biofilms in the presence of Mn^{2+} as described earlier. After 48 h, biofilms were stained with 0.05% Calcofluor solution.

To assess viability, biofilms were stained with the LIVE/DEAD BacLight Viability Kit according to the manufacturer's instruction. Biofilms were observed from the bottom of the microtiter plate under an Olympus FV1000 confocal microscope. ImageJ was used for analyzing images (Schneider, Rasband and Eliceiri 2012).

Bioinformatic analysis

Bcr1 from *Candida orthopsilosis* (XP_003869584.1), *Candida viswanathii* (XP_026591228.1), *C. tropicalis* (XP_002545827.1), *Candida dubliniensis* (XP_002422159.1), *C. albicans* (KHC28444.1) and *Lodderomyces elongisporus* (XP_001525195.1) were identified by a Blast search (National Center for Bioinformatic Information) with Bcr1 (CCE42957.1) from *C. parapsilosis*. The proteins were aligned by Clustal using standard parameters. The alignment was visualized with the sequence alignment editor BioEdit (http://www.mbio.ncsu.edu/BioEdit/bioedit.html).

RESULTS

Impact of different transition metal ions on biofilm forming ability of *C. parapsilosis*

Thirty-three epidemiologically unrelated strains of *C. parapsilosis* from bloodstream infection had been categorized into no, low and high biofilm forming phenotypes according to their performance on different surfaces such as a silicone elastomer and a polystyrene surface (Pannanusorn, Fernandez and Römling 2013; Pannanusorn *et al.* 2014). The categorization of these strains was initially based on quantification of biofilms by the XTT reduction assay (Pannanusorn, Fernandez and Römling 2013). Microscopic assessment of no biofilm formers showed occasional adherence of single yeast cells to the surface in contrast to low biofilm formers, which formed clusters of yeast cell. Most high biofilm formers built a differentiated biofilm composed of dense cell clusters consisting of yeast and pseudohyphae, so-called spider-like biofilm, after 48 h of growth (Pannanusorn, Fernandez and Römling 2013; Pannanusorn *et al.* 2014). To study the impact of transition metal ions on the biofilm forming ability of *C. parapsilosis*, we selected isolates with no (SMI 416), low (SMI 706) and high (SMI 828) biofilm forming abilities to investigate the impact of Co^{2+}, Cu^{2+}, Fe^{3+}, Mn^{2+}, Ni^{2+} and Zn^{2+} on biofilm formation at 30 and 37°C. Strains were grown in polystyrene 96-well microtiter plates in YNB/2% glucose medium and crystal violet staining was used to assess biofilm formation. Increasing concentrations of Co^{2+}, Cu^{2+}, Fe^{3+}, Ni^{2+} and Zn^{2+} from 0.1 to 10 mM in the growth medium led to a decrease in the biofilm forming ability of SMI 416, SMI 706 and SMI 828 at 30 and 37°C after 48 h (Fig. S1, Supporting Information). A similar decrease was observed in the case of Mn^{2+} at 37°C after 48 h (Fig. S2A, C and D, Supporting Information). However, after 48 h at 30°C, we consistently observed a concentration-dependent increase in the ability to form a biofilm, statistically significant already at 0.1–0.2 mM Mn^{2+} in no and low biofilm forming strains with a maximum at 2 mM Mn^{2+} (Fig. 1A, C and D). Interestingly, the effect was most pronounced in no and low biofilm forming strains, with a 4-fold increase in the biofilm forming ability of the no biofilm forming strain SMI 416 at 2 mM Mn^{2+} (Fig. 1A). To further elucidate the role of Mn^{2+} in the enhancement of biofilm formation of no and low biofilm formers, we investigated the impact of Mn^{2+} on the biofilm forming ability of the *C. parapsilosis* reference strain ATCC 22019, a poor biofilm former. No change in the biofilm
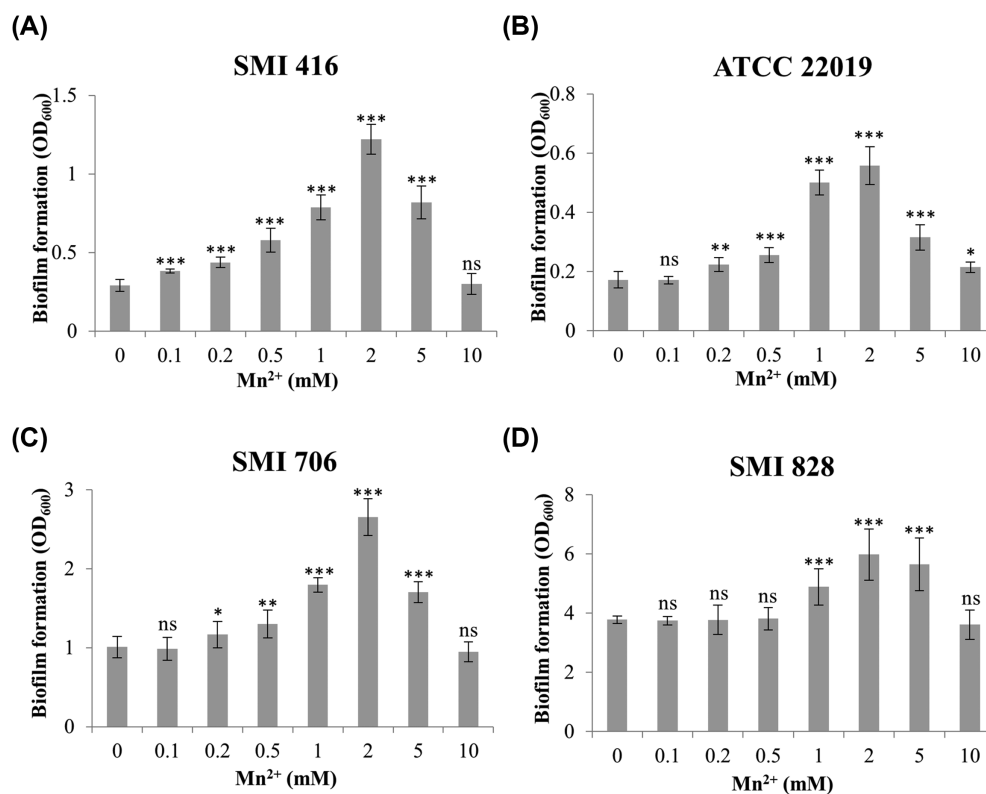
Figure 1. Impact of increasing concentration of Mn^{2+} on the biofilm forming ability of no (SMI 416 and ATCC 22019), low (SMI 706) and high (SMI 828) biofilm formers of *C. parapsilosis* on a polystyrene surface in YNB/2% glucose medium after 48 h at 30°C. **(A)** SMI 416, **(B)** ATCC 22019, **(C)** SMI 706 and **(D)** SMI 828. Values are the mean of three independent experiments conducted in three biological replicates. Error bars indicate standard deviation. Statistical significance of the differences in biofilm formation in the presence of Mn^{2+} compared to 0 mM Mn^{2+} was determined by one-way ANOVA (ns—not significant, *$P < 0.05$, **$P < 0.01$ and ***$P < 0.001$).

forming ability of ATCC 22019 was observed at 37°C upon addition of Mn^{2+} (Fig. S2B, Supporting Information). However, an ∼3-fold increase in the biofilm forming ability of ATCC 22019 was observed with 2 mM Mn^{2+} at 30°C (Fig. 1B). These data indicated a putative positive role of Mn^{2+} in biofilm formation of *C. parapsilosis* at 30°C especially in the case of the no and low biofilm forming strains SMI 416, ATCC 22019 and SMI 706.

To investigate whether the effect of Mn^{2+} on biofilm formation extended to other no biofilm forming strains, we tested the impact of 2 mM Mn^{2+} on the biofilm forming capacity of additional six clinical isolates of *C. parapsilosis*, SMI 501, SMI 630, SMI 661, SMI 681, SMI694 and SMI 798, at 30°C. Consistent with previous observations, the presence of 2 mM Mn^{2+} in the medium led to a variable, but statistically significant increase in the biofilm forming capacity of five *C. parapsilosis* clinical isolates (Fig. S3, Supporting Information). No change in the biofilm forming ability of SMI 798 in the presence of 2 mM Mn^{2+} was observed.

Impact of Mn^{2+} on the cell morphology of *C. parapsilosis*

Enhanced biofilm formation in *C. parapsilosis* is associated with a change in cell clustering and differentiation (Pannanusorn *et al.* 2014). Subsequently, biofilm formation was assessed with light microscopy to investigate biofilm morphology and cell differentiation. Biofilms of no (ATCC 22019 and SMI 416), low (SMI 706) and high (SMI 828) biofilm formers of *C. parapsilosis* were grown without and with 2 mM Mn^{2+} to achieve a maximum increase in biofilm formation at 30°C. Consistent with previously published observations (Pannanusorn *et al.* 2014), without Mn^{2+}, no biofilm forming strains did not show formation of microcolonies, but

SMI 416 occasionally attached to the surface as a single yeast cell, while ATCC 22019 formed elongated cells and clusters of two to three cells (Fig. 2). Supplementation of the medium with 2 mM Mn^{2+} led to a dramatic morphological change in the biofilm of SMI 416 and ATCC 22019 strains; increased biofilm formation was accompanied by cells to attach as smaller and extended cell clusters to the polystyrene surface and to morphologically differentiate into yeast and pseudohyphal cells (Fig. 2). Similarly, the biofilm of the low biofilm forming strain SMI 706 consisted of individually attached yeast cells, smaller and larger, mainly yeast cell clusters with the occasional formation of pseudohyphae (Pannanusorn *et al.* 2014). Upon addition of 2 mM Mn^{2+} to the YNB/2% glucose medium, SMI 706 developed a biofilm consisting mainly of extended cell clusters comprised of yeast and pseudohyphal cells (Fig. 2). The high biofilm forming strain SMI 828 developed a differentiated biofilm comprised of yeast and pseudohyphae under all investigated conditions with no major change in biofilm morphology observed upon addition of 2 mM Mn^{2+} (Fig. 2). These data suggest that the presence of enhanced concentrations of Mn^{2+} in the medium promotes biofilm formation and the development of pseudohyphae especially in no and low biofilm forming strains.

Having established the association between enhanced crystal violet staining and the amount of biofilm, we were subsequently wondering at which stage in the biofilm development, upon initial attachment and/or development of a mature biofilm, Mn^{2+} exerts its effect. To study the impact of Mn^{2+} on initial attachment, we allowed the adherence of *C. parapsilosis* SMI 416 and ATCC 22019 cells to the polystyrene surface of 96-well microtiter plates in YNB/2% glucose without and with 2 mM
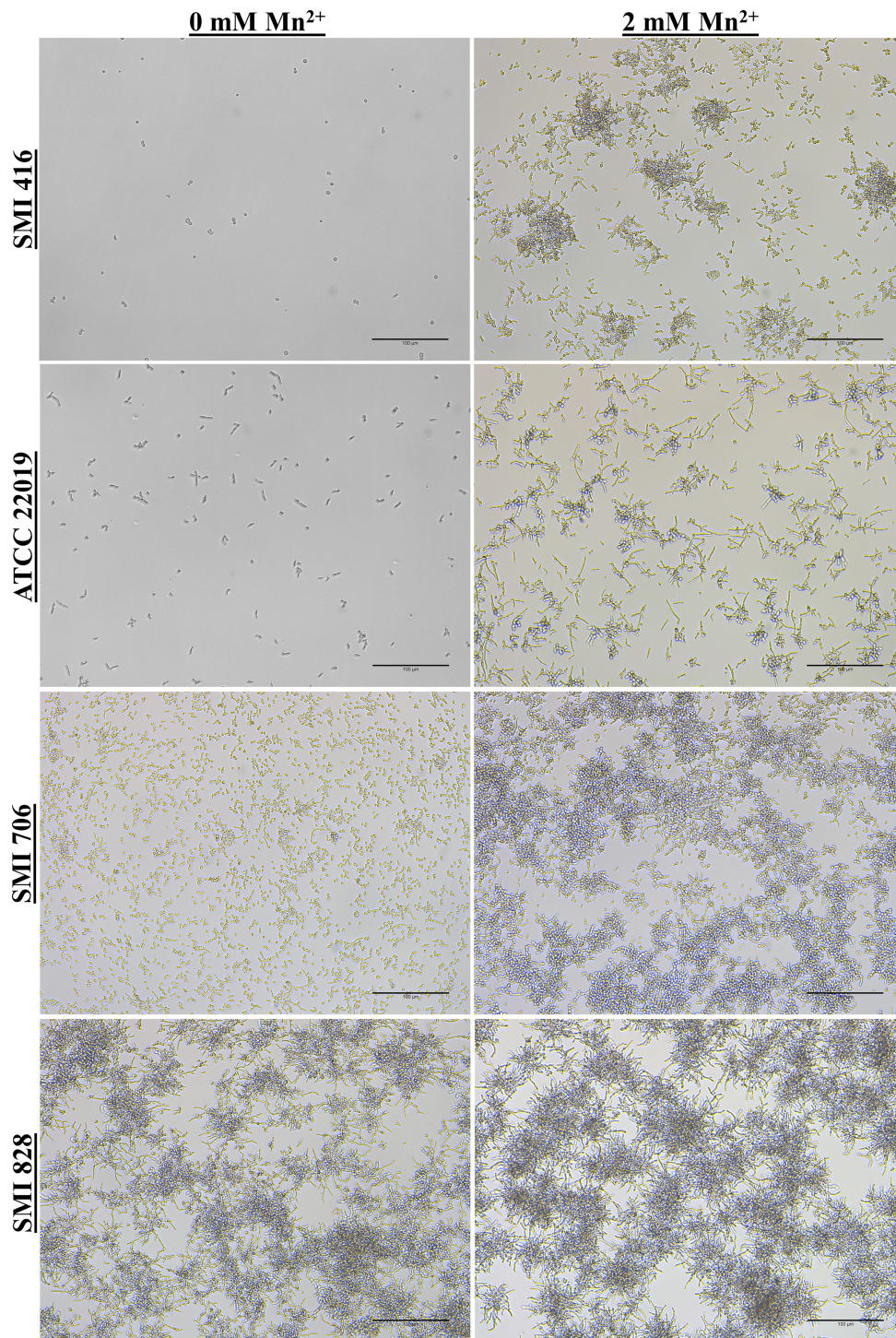
Figure 2. Impact of Mn^{2+} on biofilm formation and cell morphology on a polystyrene surface of no (SMI 416 and ATCC 22019), low (SMI 706) and high (SMI 828) biofilm formers of *C. parapsilosis* at 30°C. Scale bar represents 100 μm.

Mn^{2+} at 30°C for 3 h. Crystal violet staining indicated no difference in attachment of SMI 416 and ATCC 22019 cells to the polystyrene surface without and with 2 mM Mn^{2+} (Fig. S4, Supporting Information). These data indicate that Mn^{2+} must play a role at a later stage of biofilm formation in the no biofilm forming strains SMI 416 and ATCC 22019.

In addition, we investigated the impact of Mn^{2+} on the growth of SMI 416. The OD_{600} of SMI 416 after 48 h of growth in the presence of 2 mM Mn^{2+} was 50% lower (data not shown). Microscopic observation of SMI 416 in liquid culture indicated only yeast cells, while in the presence of 2 mM Mn^{2+} formation of small aggregates of <10 cells with hardly any single cell was observed (data not shown). We further tested cell viability of the biofilm formed by SMI 416 in the presence of 2 mM Mn^{2+} at 30°C after 48 h. Most cells in the Mn^{2+}-triggered biofilm formed by SMI 416 were viable (Fig. S5, Supporting Information).

(A)

(B)
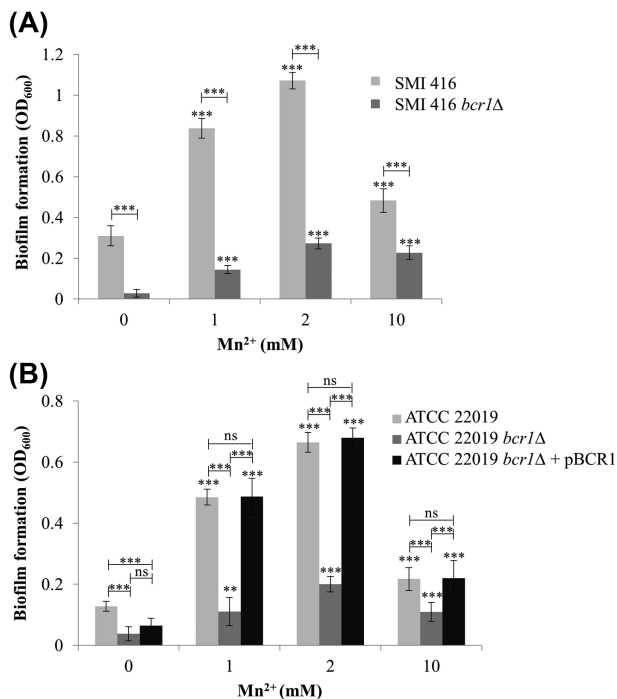
Figure 3. Impact of different concentrations of Mn^{2+} on the biofilm forming ability of wild-types SMI 416 and ATCC 22019, $bcr1\Delta$ mutants SMI 416 $bcr1\Delta$ and ATCC 22019 $bcr1\Delta$, and BCR1 complementation ATCC 22019 $bcr1\Delta$ + pBCR1 on a polystyrene surface in YNB/2% glucose medium at 30°C after 48 h. Values are the mean of three independent experiments conducted in three biological replicates. Error bars indicate standard deviation. Statistical significance of the differences in biofilm formation in the presence of Mn^{2+} compared to the absence of Mn^{2+} and wild-type compared to $bcr1\Delta$ mutant/BCR1 complementation was determined by one-way ANOVA (ns—not significant, $**P < 0.01$ and $***P < 0.001$).

Role of BCR1 in Mn^{2+}-dependent biofilms of no biofilm forming *C. parapsilosis*

Bcr1 is a major regulator of biofilm formation in low biofilm forming strains of *C. parapsilosis* (Ding and Butler 2007; Pannanusorn *et al.* 2014). To investigate a potential impact of *BCR1* deletion on Mn^{2+}-dependent biofilm formation in the no biofilm forming strains SMI 416 and ATCC 22019, we compared development of wild-type biofilms with the respective $bcr1\Delta$ mutants on a polystyrene surface in 96-well microtiter plates in the presence of different concentrations of Mn^{2+} (0, 1, 2 and 10 mM) at 30 and 37°C. No substantial change in biofilm formation between the wild-types and $bcr1\Delta$ mutants was observed at 37°C at any Mn^{2+} concentration (Fig. S6, Supporting Information). However, Mn^{2+}-dependent biofilm formation of no biofilm forming strains SMI 416 and ATCC 22019 was dramatically decreased in the absence of *BCR1* at 30°C at all investigated Mn^{2+} concentrations (Fig. 3), while complementation of *BCR1* in the ATCC 22019 strain restored Mn^{2+}-dependent biofilm formation (Fig. 3B). These data indicate that Mn^{2+}-dependent biofilm formation in the no biofilm forming strains ATCC 22019 and SMI 416 is dependent on *BCR1*.

Biofilm formation of SMI 416 $bcr1\Delta$ increased in the presence of 2 mM Mn^{2+} around 9-fold compared to YNB/2% glucose medium without added Mn^{2+} (Fig. 3A), while the relative increase in biofilm formation of the wild-type SMI 416 was around 5-fold. Similar results were observed for the reference strain ATCC 22019 (Fig. 3B). These data indicate that enhanced

biofilm formation of no biofilm formers associated with elevated Mn^{2+} concentrations is suppressed by *BCR1*.

Role of BCR1 in Mn^{2+}-dependent cell morphology of no biofilm forming *C. parapsilosis*

Subsequently, we explored the impact of the *BCR1* deletion on cell morphology of no biofilm forming strains SMI 416 and ATCC 22019 without and with 2 mM of Mn^{2+} at 30°C. Biofilm formation was observed under the light microscope after 48 h of development. While the effect of *BCR1* on cell differentiation was moderate without Mn^{2+}, in the presence of 2 mM Mn^{2+}, the $bcr1\Delta$ mutants of no biofilm forming strains SMI 416 (Fig. 4) and ATCC 22019 (Fig. 5), although significantly reduced in amount, showed biofilms comprised of yeast and pseudohyphal cells. In addition, we observed for the first time hyphae-like cells in *C. parapsilosis* biofilms. These hyphal-like cells are extensively elongated compared to pseudohyphal cells and have a reduced and uniform width (Figs 6 and 7; Fig. S7, Supporting Information). Upon complementation with *BCR1*, the $bcr1\Delta$ mutant of ATCC 22019 developed again a wild-type-like biofilm comprised of yeast and pseudohyphal cells in the presence of 2 mM Mn^{2+} (Fig. 5). These results indicate a role of *BCR1* in hyphal development in *C. parapsilosis* in the presence of Mn^{2+}.

We further investigated the impact of the *BCR1* deletion on attachment of no biofilm forming strains SMI 416 and ATCC 22019 without and with 2 mM Mn^{2+} at 30°C after 3 h. Crystal violet staining showed no difference in attachment of the $bcr1\Delta$ mutants of SMI 416 and ATCC 22019 without and with 2 mM Mn^{2+}, as observed for the wild-type. Thus, without Mn^{2+} equally as in the presence of 2 mM Mn^{2+}, a >3-fold decrease in attachment of the $bcr1\Delta$ mutants compared to the wild-type of SMI 416 and ATCC 22019 was observed (Fig. S4, Supporting Information). Thus, initial reduction in attachment contributes to reduced biofilm formation of the $bcr1\Delta$ mutants of SMI 416 and ATCC 22019 compared to their respective wild-types in Mn^{2+}-triggered biofilm formation.

Impact of media composition on BCR1-dependent cell morphology of no biofilm forming *C. parapsilosis* in the presence of Mn^{2+}

To elucidate the role of different media in the cell morphology in biofilm formation on a polystyrene surface in the presence of 2 mM Mn^{2+}, wild-type SMI 416 and its $bcr1\Delta$ mutant were grown in commonly used media (Spider, YPD and RPMI) supplemented with 2% glucose without and with 2 mM Mn^{2+} at 30°C. In YPD/2% glucose medium, SMI 416 was composed of yeast cells, while addition of 2 mM Mn^{2+} caused induction of pseudohyphae (Fig. 8). Interestingly, SMI 416 $bcr1\Delta$ showed extended hyphal development in the absence and presence of Mn^{2+} in the same medium (Fig. 8). In Spider and RPMI media, no change in cell morphology between the wild-type SMI 416 and its $bcr1\Delta$ mutant was observed in the presence or absence of 2 mM Mn^{2+} (data not shown). These data indicate medium-specific hyphal development in the absence of *BCR1* in the no biofilm forming clinical isolate SMI 416.

DISCUSSION

In a previous study, 33 clinical isolates of *C. parapsilosis* from bloodstream infection were categorized into no, low and high
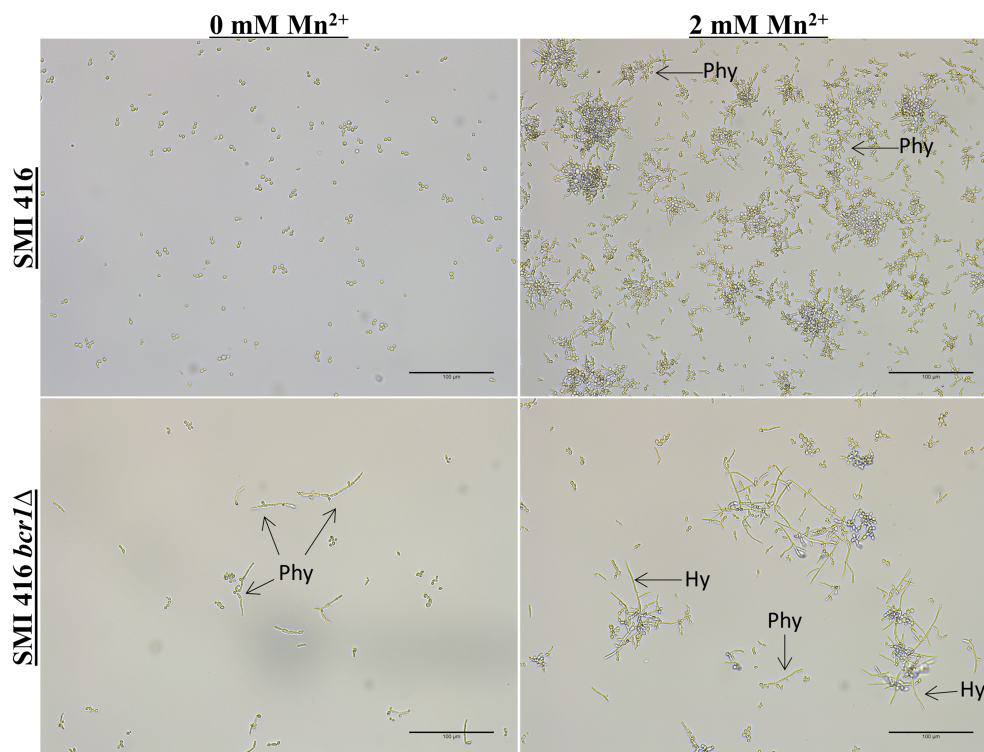
Figure 4. Impact of the *BCR1* deletion on biofilm formation and cell morphology of wild-type *C. parapsilosis* SMI 416 and its *bcr1Δ* mutant at 30°C on a polystyrene surface in YNB/2% glucose medium with 0 and 2 mM of Mn^{2+}. Arrows indicate pseudohyphae (Phy) and hyphae (Hy). Scale bar represents 100 μm.

based on their biofilm forming ability (Pannanusorn, Fernandez and Römling 2013; Pannanusorn *et al*. 2014). Here, we show that Mn^{2+} positively affects biofilm formation of clinical isolates with no and low biofilm forming ability at 30°C. Furthermore, Mn^{2+} has a pronounced effect on cell morphology, especially in the absence of *BCR1*, triggering pseudohyphae and hyphae formation in no biofilm formers.

All forms of life require various metal ions as cofactors playing a structural and catalytic role in macromolecules involved in various fundamental biological processes. The transition metal ions Co^{2+}, Cu^{2+}, Fe^{3+}, Mn^{2+}, Ni^{2+} and Zn^{2+} are required by most organisms, as they are involved in essential physiological processes, but are toxic at higher concentrations. We tested the impact of these transition metal ions on biofilm formation of *C. parapsilosis* isolates with different biofilm forming ability at 30 and 37°C. Most of the metal ions reduced biofilm formation in *C. parapsilosis* clinical isolates independent of temperature and the biofilm forming capacity of the strains (Supporting Information). Surprisingly, in case of Mn^{2+} at 30°C, we observed enhanced biofilm formation of strains previously categorized to make no biofilm in YNB/2% glucose medium. The amount of biofilm formed by no biofilm forming strains in the presence of 2 mM Mn^{2+} corresponded to the amount of biofilm formed by the low biofilm forming strain SMI 706. In the presence of 2 mM Mn^{2+}, we, however, observed enhanced development of pseudohyphae in no biofilm formers of *C. parapsilosis*. The role of metal ions in biofilm formation of *C. albicans* and *C. tropicalis* was previously investigated (Harrison *et al*. 2006, 2007). Metal ions can alter the structure of the biofilm by either blocking or enhancing the transition between yeast and hyphal cell types (Harrison *et al*. 2007). For example, Pb^{2+} in *C. albicans* and Zn^{2+} and CrO_4^{2-} in *C. tropicalis* were observed to trigger hyphal formation (Harrison *et al*. 2007).

Biofilm formation is a major virulence factor of *Candida* species that is regulated by a network of transcription factors, which affects adhesion, hyphal formation and the production of extracellular polymeric substances (Cavalheiro and Teixeira 2018). Screening a mutant library of 165 transcriptional regulators identified six transcription factors *BCR1*, *BRG1*, *EFG1*, *NDT80*, *ROB1* and *TEC1* to affect biofilm formation of *C. albicans* on rat denture and in catheter models (Nobile *et al*. 2012). This highly complex regulatory network of different transcriptional regulators promotes the expression of a high number of target genes with overlapping target promoters for several transcriptional regulators (Nobile *et al*. 2012). In *C. parapsilosis*, overlapping transcription factor networks for *ACE2*, *BCR1*, *EFG1* and *UME6* to regulate biofilm formation in *C. parapsilosis* have been established (Ding and Butler 2007; Connolly *et al*. 2013; Holland *et al*. 2014). We demonstrated previously that *BCR1* promotes biofilm formation of all low, and one of two high filamentous, biofilm forming *C. parapsilosis* clinical isolates, but does not play a role in, or even enhances, biofilm formation of high biofilm forming clinical isolates with spider-like biofilm morphology (Pannanusorn *et al*. 2014). Thus, *BCR1* can have different roles in biofilm formation in the same species. Here, we show that *BCR1* activates biofilm formation also in the no biofilm forming isolates SMI 416 and ATCC 22019 upon Mn^{2+}-dependent enhancement of biofilm formation. This Mn^{2+}-dependent effect on biofilm formation has a *BCR1*-dependent and -independent component indicating the importance of environmental conditions that alter regulation of biofilm formation by various transcription factors.

To colonize and form biofilm at a surface, *C. parapsilosis* initially adheres as single cells and subsequently builds up microcolonies (Pannanusorn *et al*. 2014). The initial adherence of *Candida* cells is an important factor for dissemination of the *Candida* infection and regulated by different environmental conditions, the host and the physiological status of the *Candida* cell
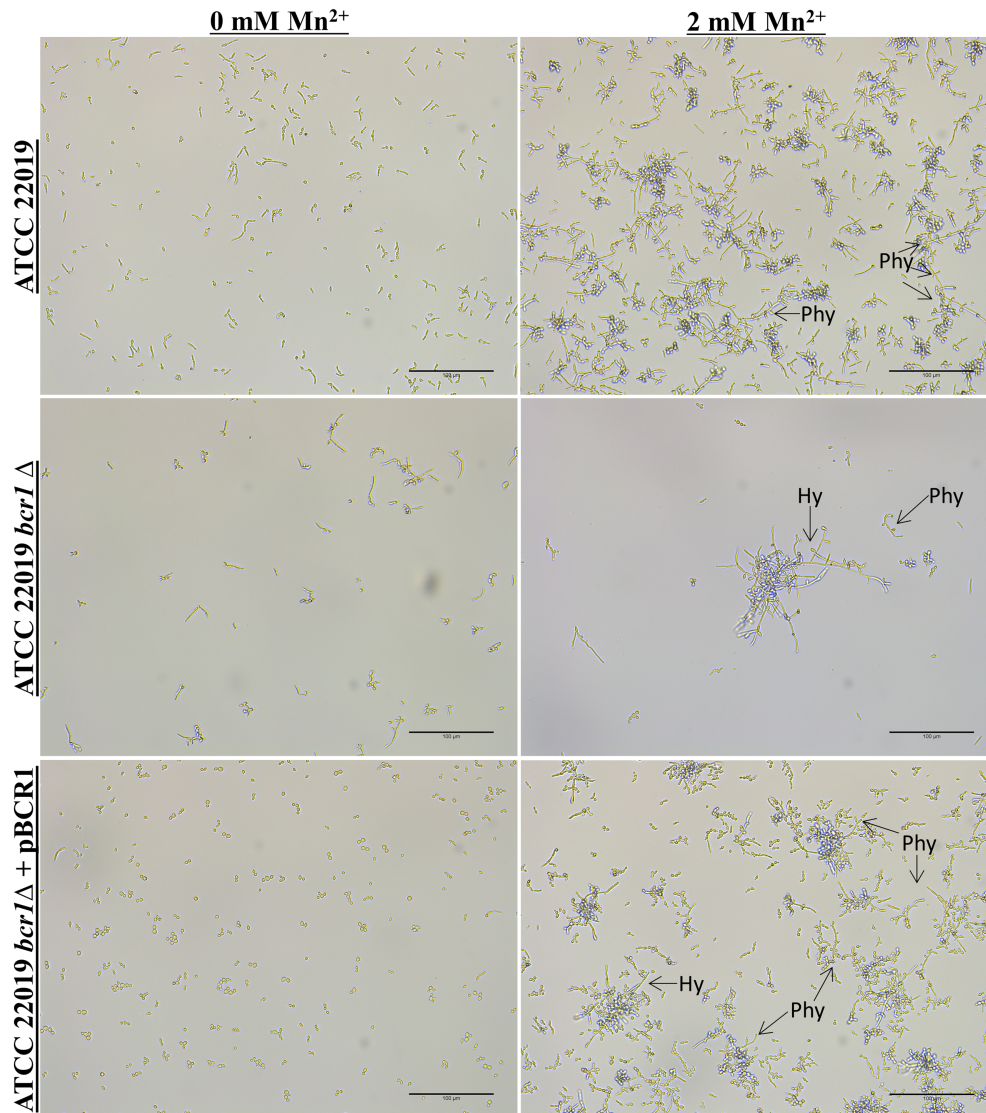
Figure 5. Impact of *BCR1* deletion on biofilm formation and cell morphology of C. *parapsilosis* ATCC 22019 wild-type, its *bcr1*Δ mutant and *BCR1* complementation at 30°C on a polystyrene surface in YNB/2% glucose medium with 0 and 2 mM of Mn^{2+}. Arrows indicates the presence of pseudohyphae (Phy) and hyphae (Hy). Scale bar represents 100 μm.

(Silva *et al.* 2011; Araújo, Henriques and Silva 2017). *Candida* possesses different cell wall proteins for this adherence process (Silva *et al.* 2011; Araújo, Henriques and Silva 2017). *BCR1* is involved in cell adhesion of low and high biofilm forming isolates (Bastidas, Heitman and Cardenas 2009; Pannanusorn *et al.* 2014; Araújo, Henriques and Silva 2017). The presence of Mn^{2+}, though, has no effect on the initial *BCR1*-dependent adhesion indicating that this stage of biofilm formation is not affected by Mn^{2+}.

One of the important factors for virulence of *C. albicans* is the ability to switch between the different cell morphologies: yeast, pseudohyphae and hyphae (Sudbery, Gow and Berman 2004). This morphology switch is important for colonization, tissue penetration and invasion (Gow, Brown and Odds 2002; Trevijano-Contador, Rueda and Zaragoza 2016). Pseudohyphae and hyphae are invasive, but pseudohyphae may have different role and properties compared to hyphae during infection (Sudbery, Gow and Berman 2004). *Candida parapsilosis* is believed

to not form true hyphae, but to exist in either a yeast or a pseudohyphal form. We show in this work that no biofilm forming strains, which otherwise adhere as single cells, develop biofilms comprised of yeasts and pseudohyphae in the presence of Mn^{2+}. Deletion of *BCR1* in these no biofilm formers led to development of hyphae on the polystyrene surface, predominantly Mn^{2+}-triggered biofilm formation. Thus, *BCR1* is a repressor of hyphal development in initially no biofilm forming strains, while *BCR1* contributes to extended pseudohyphal formation in high spider-like biofilm forming strains (Pannanusorn *et al.* 2014).

The different cell morphologies observed in surface biofilms of *C. parapsilosis*, yeast (blastospore and budding yeast), pseudohyphae and hyphae (germ tube and hyphae), are shown in Fig. 7. Although hyphae and pseudohyphae are both filamentous in morphology (Thompson, Carlisle and Kadosh 2011), clear morphological differences exist between hyphae and pseudohyphae. Hyphae are uniform in width with no constriction at the
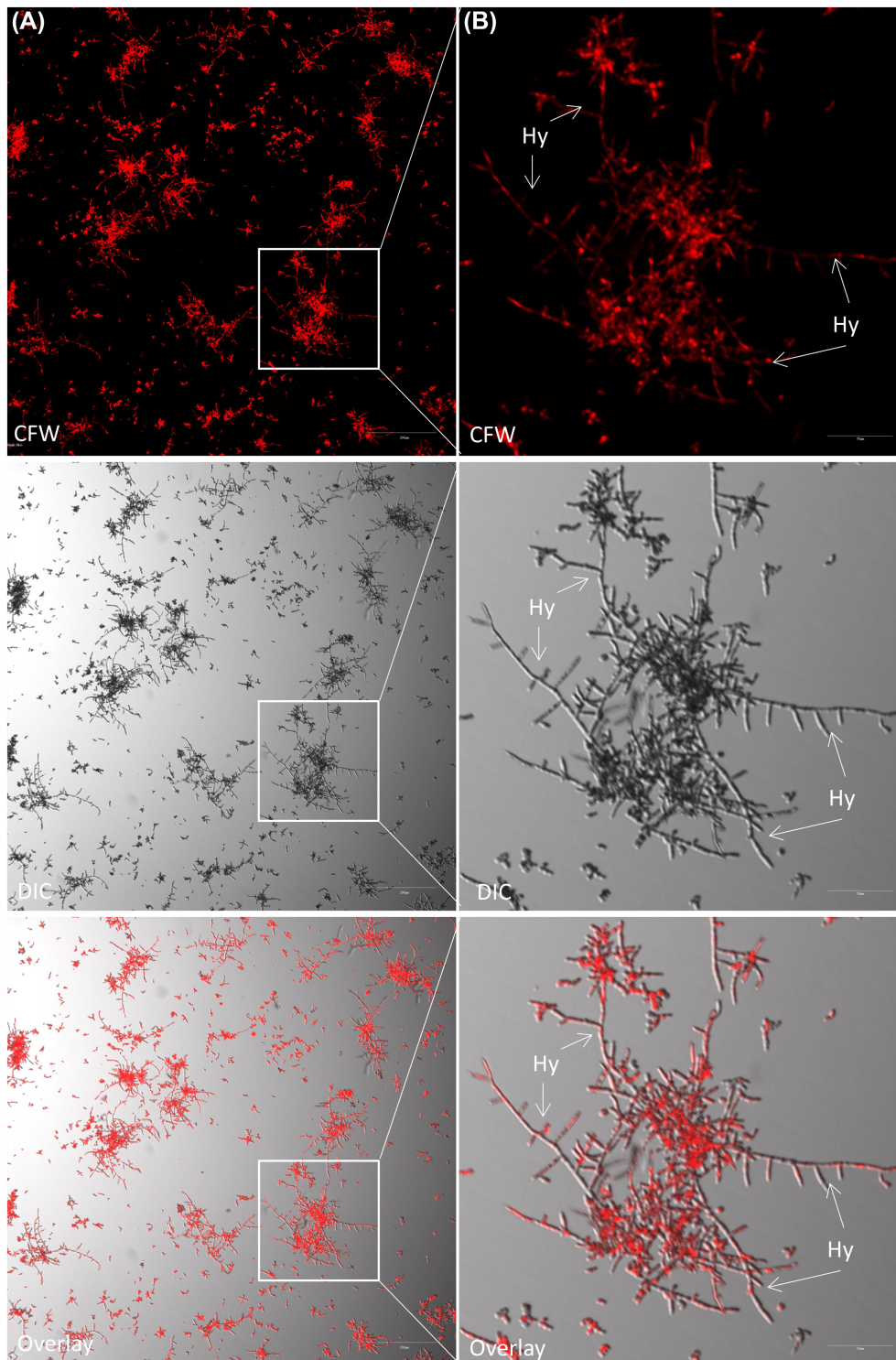
Figure 6. Visualization of hyphal development in the *bcr1∆* mutant of *C. parapsilosis* SMI 416 at 30°C on a polystyrene surface in YNB/2% glucose medium with 2 mM Mn^{2+}. Arrows indicate the presence of hyphae (Hy). Scale bars: **(A)** 200 μm and **(B)** 50 μm.

neck of mother cell (Fig. 7F–H; Fig. S7B–D, Supporting Information), while pseudohyphae are wider and have a clear constriction at the neck of the mother cell (Fig. 7E; Fig. S7A, Supporting Information) (Sudbery, Gow and Berman 2004). In *C. albicans*, the width of hyphal cells is around 2 μm, while pseudohyphal cells are around 2.8 μm (Sudbery, Gow and Berman 2004). Regulation

of hyphal development in *C. parapsilosis* requires further investigations, but key genes involved in hyphal formation are present in the *C. parapsilosis* genome (Fig. 9).

Major transcriptional regulators of biofilm formation can direct other physiological processes, including hyphal differentiation (Cavalheiro and Teixeira 2018). Bcr1 is involved in regulation of opaque cell filamentation in *C. albicans* (Guan *et al*. 2013).
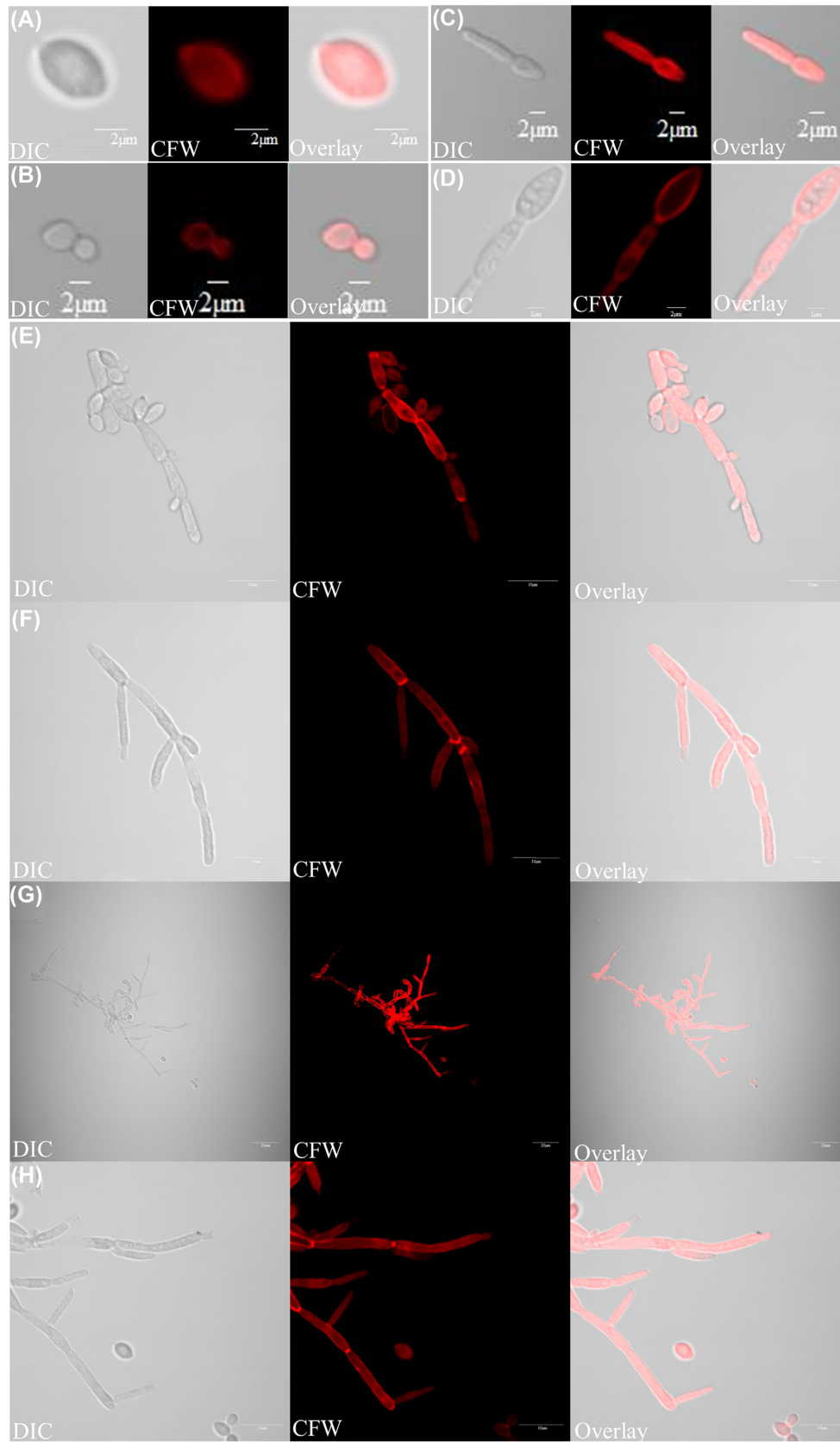
Figure 7. Different cell morphologies observed in this study: **(A)** blastospore, **(B)** budding yeast, **(C, D)** germ tube, **(E)** pseudohyphae and **(F–H)** hyphae. Light (left) and fluorescent (Calcofluor staining; middle) microscopy images of different cell types were overlaid (right). Scale bars: (A–D) 2 μm, (E, F, H) 10 μm and (G) 20 μm.
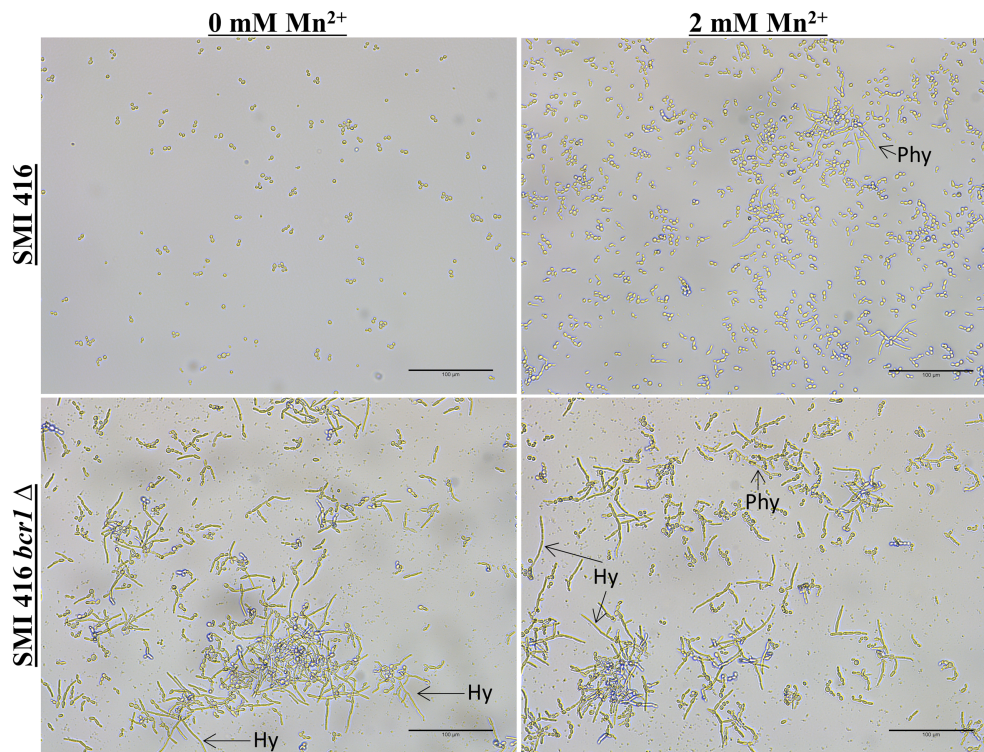
Figure 8. YPD/2% glucose medium induces filamentous growth of *C. parapsilosis* SMI 416 in a polystyrene surface. Cell morphology of *C. parapsilosis* SMI 416 wild-type and *bcr1Δ* mutant in YPD/2% glucose medium with and without 2 mM Mn^{2+} at 30°C. Scale bar represents 100 μm.
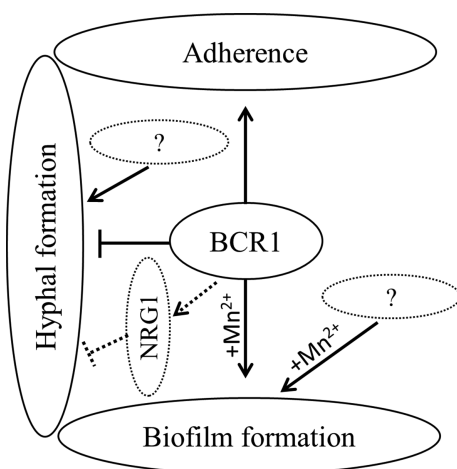
Figure 9. A tentative model of the role of Bcr1 in no biofilm forming isolates of *C. parapsilosis*.

The role of the transcription factor Nrg1 has not been defined in *C. parapsilosis* (Pais *et al.* 2016). Nrg1 represses the filamentous growth in *C. albicans* and *C. tropicalis* (Braun, Kadosh and Johnson 2001; Zhang *et al.* 2016). Bcr1, which directly represses the *NRG1* promoter (Nobile *et al.* 2012; Guan *et al.* 2013), does not play a role in regulation of hyphal development. However, *BCR1* activates genes encoding hyphal surface proteins during biofilm formation (Nobile and Mitchell 2005). Here, we observed a high number of pseudohyphae and hyphae (filamentous forms) in biofilms formed by the *bcr1Δ* mutants in Mn^{2+}-triggered biofilm formation of no biofilm forming strains of *C. parapsilosis*. Possibly, deletion of *BCR1* abolishes expression of *NRG1*, which, in combination with rewiring of the regulatory circuit, relieves repression on

filamentous growth in surface-attached cells of Mn^{2+}-triggered biofilm formation of no biofilm formers of *C. parapsilosis* (Fig. 9). The role of Nrg1, its regulation by Bcr1 and the Bcr1 network require further investigation in these clinical isolates of *C. parapsilosis*.

In summary, Bcr1 has at least three different functionalities in *C. parapsilosis* in no, low and high biofilm forming strains with respect to biofilm formation and plasticity in cell morphology leading to pseudohyphae and hyphae development. Bcr1 also represses protease activity and contributes to antimicrobial peptide resistance and altered colony and cell morphology (Pannanusorn *et al.* 2014). But what can be the molecular basis of the differential activities of Bcr1 in the different categories of biofilm forming strains of *C. parapsilosis* and *C. albicans*? In *C. albicans*, network circuit diversification leading Bcr1 to differentially control the transcription factor Brg1 is partially responsible for differential regulation of biofilm and cell morphology (Huang *et al.* 2019). Nucleotide sequence variation in promoter regions of target genes and Bcr1 as a target for extensive post-translational modification can be the cause of circuit diversification. Bcr1 is a complex 724 amino acid long invariant transcription factor in *C. parapsilosis* with tandem highly conserved C2H2 zinc finger repeats (188–218 and 219–247) flanked by lysine-rich sequences (Fig. S8, Supporting Information). Otherwise, Bcr1 is predicted to consist of 84% disordered sequences with compositional bias toward serine, glutamine and proline, which make up over 40% of the amino acids of the protein. Besides *C. parapsilosis*, Bcr1 homologues are found in *C. orthopsilosis*, *C. viswanathii*, *C. tropicalis*, *C. dubliniensis*, *C. albicans* and *L. elongisporus*. Homology outside the C2H2 zinc finger motifs is below 45% with gaps with extended amino acid stretches.

Most of Bcr1 functionality is known in *C. albicans* where Bcr1 expression and activity is highly regulated. For example, the

hyphal regulator Tec1 activates and Tup1 represses *BCR1* expression (Gutiérrez-Escribano *et al.* 2012). Furthermore, phosphorylation of Bcr1 of *C. albicans* at threonine 191 and serine 556 by the serine/threonine protein kinase Cbk1 is required for transcriptional activity (Gutiérrez-Escribano *et al.* 2012). A Cbk1 homologue with 77% homology is also present in *C. parapsilosis* (data not shown). Threonine 191 present in C2H2 zinc finger repeats is highly conserved in Bcr1 of all species (Fig. S8, Supporting Information). However, absence of serine 556 in *C. orthopsilosis* and *C. parapsilosis* can contribute to different activities of Bcr1 between *C. parapsilosis* and *C. albicans*. In summary, Bcr1 is a major stimulator of biofilm formation and a repressor of cell morphology in no biofilm forming strains dependent on environmental conditions that requires its differential role to be further investigated in *C. parapsilosis*.

SUPPLEMENTARY DATA

Supplementary data are available at FEMSYR online.

FUNDING

REFERENCES

Allison DL, Willems HM, Jayatilake JA *et al.. Candida*–bacteria interactions: their impact on human disease. *Microbiol Spectr* 2016;**4**:VMBF-0030-2016, DOI: 10.1128/microbiolspec.VMBF-0030-2016.

Araújo D, Henriques M, Silva S. Portrait of *Candida* species biofilm regulatory network genes. *Trends Microbiol* 2017;**25**:62–75.

Bastidas RJ, Heitman J, Cardenas ME. The protein kinase Tor1 regulates adhesin gene expression in *Candida albicans*. *PLoS Pathog* 2009;**5**:e1000294.

Braun BR, Kadosh D, Johnson AD. NRG1, a repressor of filamentous growth in *C. albicans*, is down-regulated during filament induction. *EMBO J* 2001;**20**:4753–61.

Cavalheiro M, Teixeira MC. *Candida* biofilms: threats, challenges, and promising strategies. *Front Med* 2018;**5**:28.

Clerihew L, Lamagni TL, Brocklehurst P *et al. Candida parapsilosis* infection in very low birthweight infants. *Arch Dis Child Fetal Neonatal Ed* 2007;**92**:F127–9.

Connolly LA, Riccombeni A, Grózer Z *et al.* The APSES transcription factor Efg1 is a global regulator that controls morphogenesis and biofilm formation in *Candida parapsilosis*. *Mol Microbiol* 2013;**90**:36–53.

Cvetkovic A, Menon AL, Thorgersen MP *et al.* Microbial metalloproteomes are largely uncharacterized. *Nature* 2010;**466**:779–82.

Ding C, Butler G. Development of a gene knockout system in *Candida parapsilosis* reveals a conserved role for BCR1 in biofilm formation. *Eukaryot Cell* 2007;**6**:1310–9.

Ding C, Vidanes GM, Maguire SL *et al.* Conserved and divergent roles of Bcr1 and CFEM proteins in *Candida parapsilosis* and *Candida albicans*. *PLoS One* 2011;**6**:e28151.

Finkel JS, Mitchell AP. Genetic control of *Candida albicans* biofilm development. *Nat Rev Microbiol* 2011;**9**:109–18.

Gow NAR, Brown AJP, Odds FC. Fungal morphogenesis and host invasion. *Curr Opin Microbiol* 2002;**5**:366–71.

Guan G, Xie J, Tao L *et al.* Bcr1 plays a central role in the regulation of opaque cell filamentation in *Candida albicans*. *Mol Microbiol* 2013;**89**:732–50.

Gutiérrez-Escribano P, Zeidler U, Suárez MB *et al.* The NDR/LATS kinase Cbk1 controls the activity of the transcriptional regulator Bcr1 during biofilm formation in *Candida albicans*. *PLoS Pathog* 2012;**8**:e1002683.

Harrison JJ, Ceri H, Yerly J *et al.* Metal ions may suppress or enhance cellular differentiation in *Candida albicans* and *Candida tropicalis* biofilms. *Appl Environ Microbiol* 2007;**73**:4940–9.

Harrison JJ, Rabiei M, Turner RJ *et al.* Metal resistance in *Candida* biofilms. *FEMS Microbiol Ecol* 2006;**55**:479–91.

Holland LM, Schröder MS, Turner SA *et al.* Comparative phenotypic analysis of the major fungal pathogens *Candida parapsilosis* and *Candida albicans*. *PLoS Pathog* 2014;**10**:e1004365.

Huang MY, Woolford CA, May G *et al.* Circuit diversification in a biofilm regulatory network. *PLoS Pathog* 2019;**15**:e1007787.

Kuhn DM, Mikherjee PK, Clark TA *et al. Candida parapsilosis* characterization in an outbreak setting. *Emerg Infect Dis* 2004;**10**:1074–81.

Lackey E, Vipulanandan G, Childers DS *et al.* Comparative evolution of morphological regulatory functions in *Candida* species. *Eukaryot Cell* 2013;**12**:1356–68.

Mackie J, Szabo EK, Urgast DS *et al.* Host-imposed copper poisoning impacts fungal micronutrient acquisition during systemic *Candida albicans* infections. *PLoS One* 2016;**11**:e0158683.

Medrano DJ, Brilhante RS, Cordeiro RA *et al.* Candidemia in a Brazilian hospital: the importance of *Candida parapsilosis*. *Rev Inst Med Trop Sao Paulo* 2006;**48**:17–20.

Ng KP, Saw TL, Na SL *et al.* Systemic *Candida* infection in University hospital 1997–1999: the distribution of *Candida* biotypes and antifungal susceptibility patterns. *Mycopathologia* 2001;**149**:141–6.

Nobile CJ, Fox EP, Nett JE *et al.* A recently evolved transcriptional network controls biofilm development in *Candida albicans*. *Cell* 2012;**148**:126–38.

Nobile CJ, Mitchell AP. Regulation of cell-surface genes and biofilm formation by the *C. albicans* transcription factor Bcr1p. *Curr Biol* 2005;**15**:1150–5.

Odds FC. *Candida and Candidosis*. London: Tindall, 1988.

O'Toole GA. Microtiter dish biofilm formation assay. *J Vis Exp* 2011;**47**:2437, DOI: 10.3791/2437.

Pais P, Costa C, Cavalheiro M *et al.* Transcriptional control of drug resistance, virulence and immune system evasion in pathogenic fungi: a cross-species comparison. *Front Cell Infect Microbiol* 2016;**6**:131.

Pannanusorn S, Fernandez V, Römling U. Prevalence of biofilm formation in clinical isolates of *Candida* species causing bloodstream infection. *Mycoses* 2013;**56**:264–72.

Pannanusorn S, Ramírez-Zavala B, Lünsdorf H *et al.* Characterization of biofilm formation and the role of BCR1 in clinical isolates of *Candida parapsilosis*. *Eukaryot Cell* 2014;**13**:438–51.

Pfaller MA, Diekema DJ, Jones RN *et al.* International surveillance of bloodstream infections due to *Candida* species: frequency of occurrence and *in vitro* susceptibilities to fluconazole, ravuconazole, and voriconazole of isolates collected from 1997 through 1999 in the SENTRY Antimicrobial Surveillance Program. *J Clin Microbiol* 2001;**39**: 3254–9.

Pfaller MA, Moet GJ, Messer SA *et al.* Candida bloodstream infections: comparison of species distributions and antifungal resistance patterns in community-onset and nosocomial isolates in the SENTRY Antimicrobial Surveillance Program, 2008–2009. *Antimicrob Agents Chemother* 2011;**55**:561–6.

Reuss O, Vik A, Kolter R et al. The SAT1 flipper, an optimized tool for gene disruption in Candida albicans. Gene 2004;**341**:119–27.

Rodríguez J, Mandalunis PM. A review of metal exposure and its effects on bone health. J Toxicol 2018;**2018**: 4854152.

Roilides E, Farmaki E, Evdoridou J et al. Neonatal candidiasis: analysis of epidemiology, drug susceptibility, and molecular typing of causative isolates. Eur J Clin Microbiol Infect Dis 2004;**23**:745–50.

Sasse C, Morschhäuser J. Gene deletion in Candida albicans wild-type strains using the SAT1-flipping strategy. Methods Mol Biol 2012;**845**:3–17.

Schneider CA, Rasband WS, Eliceiri KW. NIH Image to ImageJ: 25 years of image analysis. Nat Methods 2012;**9**:671–5.

Silva S, Negri M, Henriques M et al. Adherence and biofilm formation of non-Candida albicans Candida species. Trends Microbiol 2011;**19**:241–7.

Sudbery P, Gow N, Berman J. The distinct morphogenic states of Candida albicans. Trends Microbiol 2004;**12**:317–24.

Thompson DS, Carlisle PL, Kadosh D. Coevolution of morphology and virulence in Candida species. Eukaryot Cell 2011;**10**:1173–82.

Tóth R, Nosek J, Mora-Montes HM et al. Candida parapsilosis: from genes to the bedside. Clin Microbiol Rev 2019;**32**:e00111-18, DOI: 10.1128/CMR.00111-18.

Trevijano-Contador N, Rueda C, Zaragoza O. Fungal morphogenetic changes inside the mammalian host. Semin Cell Dev Biol 2016;**57**:100–9.

Trofa D, Gácser A, Nosanchuk JD. Candida parapsilosis, an emerging fungal pathogen. Clin Microbiol Rev 2008;**21**:606–25.

van Asbeck EC, Clemons KV, Stevens DA. Candida parapsilosis: a review of its epidemiology, pathogenesis, clinical aspects, typing and antimicrobial susceptibility. Crit Rev Microbiol 2009;**35**:283–309.

Weems JJ. Candida parapsilosis: epidemiology, pathogenicity, clinical manifestations, and antimicrobial susceptibility. Clin Infect Dis 1992;**14**:756–66.

Wisplinghoff H, Bischoff T, Tallent SM et al. Nosocomial bloodstream infections in US hospitals: analysis of 24,179 cases from a prospective nationwide surveillance study. Clin Infect Dis 2004;**39**:309–17.

Zhang Q, Tao L, Guan G et al. Regulation of filamentation in the human fungal pathogen Candida tropicalis. Mol Microbiol 2016;**99**:528–45.